



Cite this: *Chem. Sci.*, 2025, **16**, 22091

All publication charges for this article have been paid for by the Royal Society of Chemistry

Received 12th July 2025
Accepted 13th October 2025

DOI: 10.1039/d5sc05199a
rsc.li/chemical-science

Introduction

Cysteine (Cys) plays a crucial role in biochemical transformations and enzymatic processes due to its nucleophilicity, metal-coordination ability and redox activity.¹ It is also essential for native chemical ligation, a widely used strategy in peptide and protein synthesis.² Beyond transformations exploiting the nucleophilicity of Cys,³ desulfurative modifications have emerged as powerful tools for post-assembly peptide modification and post-translational protein mutagenesis.⁴ To introduce diverse substituents while preserving α -carbon stereochemistry, various Cys desulfurization methods based on C β -S bond homolysis have been developed.

Building upon the pioneering work of the Hoffman and Walling groups,^{5,6} Wan and Danishefsky established a radical desulfurization protocol for Cys at the protein level, involving a thiophosphoranyl radical intermediate (Fig. 1A).⁷ Subsequent advances,⁸ including photochemical methods for peptide and protein desulfurization,⁹ have broadened the utility of this approach. Mitchell's group employed a related approach to introduce groups appended to a persistent radical trap

(TEMPO) and N $^{\epsilon}$ -modified side chains at the original Cys site in peptides and ubiquitin K48C.¹⁰ However, the use of photocatalysts may generate reactive oxygen species and promote undesirable photoredox side reactions.¹¹ Walczak and co-workers achieved desulfurative borylation by identifying a combination of 1,3,5-triaza-7-phosphaadamantane and tetrahydroxydiboron that served as a radical initiator and a boron source, respectively.¹² Another approach to Cys desulfurization involves the S H_2 mechanism to generate the L-alanyl C β $^{\cdot}$ radical, which is subsequently trapped by external reagents to form modified products.^{13,14} Despite its potential, this S H_2 strategy has not yet been explored in the context of proteins, particularly under biocompatible conditions.

Davis and co-workers recently developed a perfluoropyridine-based method for photo-induced C-S bond cleavage, mediated by either single electron transfer (SET) or formation of electron donor-electron acceptor (EDA) complexes.¹⁵ While this approach avoids the use of phosphines, it still requires a large excess of thiophenol as an adjuvant.

Despite the advances, there remains a need for bio-compatible methods to convert Cys into natural residues or their analogues. Notably, direct C β -S bond homolysis without external mediators remains challenging and has been rarely demonstrated, even in flask reactions. Herein, we report the discovery of a novel chromophore that facilitates this transformation *via* direct photoexcitation, obviating the need for additional reagents and expanding the scope of C(sp 3)-S bond chemistry.

We have reported that irradiation of pro-aromatic 1,4-dihydropyridazines generates C(sp 3)-centered radicals, enabling diverse dealkenylative transformations.¹⁶ Building on this work, we sought to identify heterocyclic motifs that could be readily installed onto Cys residues in aqueous solution and possess the

^aKey Laboratory of Bioorganic Chemistry and Molecular Engineering of Ministry of Education, Beijing National Laboratory for Molecular Science, College of Chemistry and Molecular Engineering, Peking University, Beijing 100871, China. E-mail: tuopingluo@pku.edu.cn

^bDepartment of Chemistry, The Hong Kong University of Science and Technology, Hong Kong 999077, China

^cInstitute of Molecular Physiology, Shenzhen Bay Laboratory, Shenzhen, Guangdong 518055, China

^dPeking-Tsinghua Center for Life Sciences, Academy for Advanced Interdisciplinary Studies, Peking University, Beijing 100871, China

† These authors contributed equally.



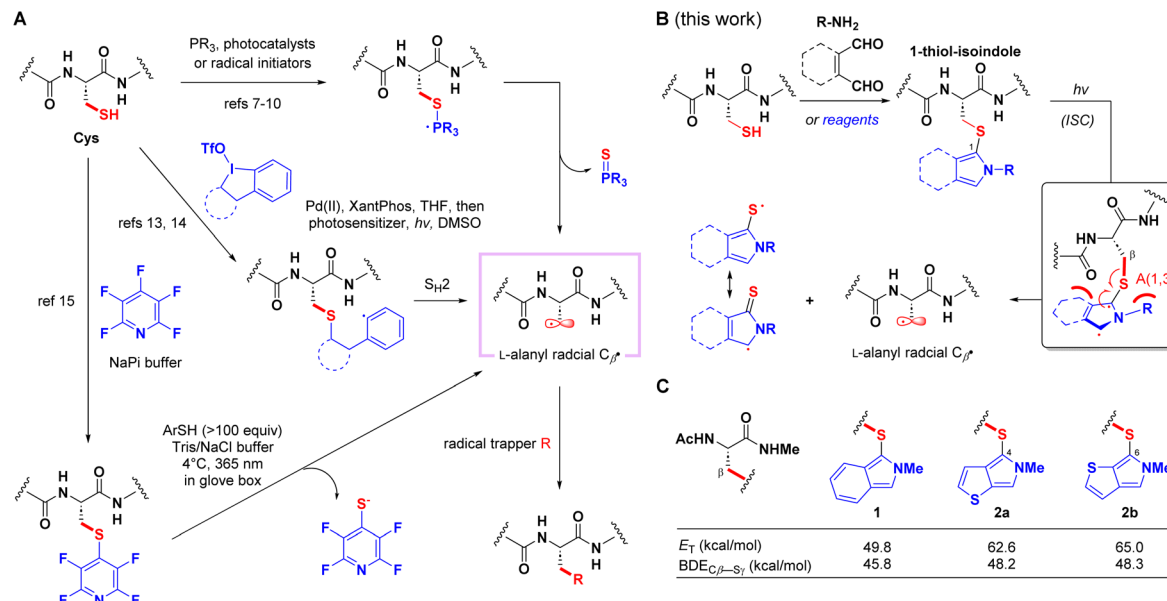


Fig. 1 Previous methods for radical desulfurative modifications of cysteine and the approach proposed in this study. (A) Phosphine-assisted desulfurization via phosphoranyl radicals, S_2H strategy, and thiol activation through photoinduced electron transfer to fluoropyridines. (B) The postulated photo-induced $\text{C}_\beta\text{-S}$ bond homolysis based on the isoindole chromophore. (C) DFT calculations of three different chromophores; energy obtained at the (U)ωB97X-D/def2 TZVP/SMD(H2O)/(U)ωB97X-D/def2-SVP/SMD(H2O) level.

potential for C-S homolysis upon photoexcitation. We were particularly drawn to the three-component reaction (3CR) involving a thiol, an amine and *ortho*-phthalaldehyde (OPA), which forms 1-thiol-isoindoles or similar heterocycles.¹⁷ This 3CR has been applied in various scenarios, including amino acid detection,¹⁸ cross-linking of kinase–substrate pairs,¹⁹ peptide stapling,²⁰ and peptide–peptide conjugates.²¹ Meanwhile, the photoreactivity of the fluorescent isoindole species has not been explored to the best of our knowledge. We envisaged that the $\text{C}_\beta\text{-S}$ bond in these compounds (highlighted in red) could adopt a conformation perpendicular to the π -system to minimize A(1,3)-interactions (allylic 1,3-strain),²² and therefore direct photo-excitation might lead to the formation of L-alanyl $\text{C}_\beta\cdot$ radicals *via* homolysis, presumably from the triplet state, which has a longer life than that of the singlet state (Fig. 1B). Consequently, we performed DFT calculations on three model compounds (**1** and **2a/b**) (Fig. 1C). While the predicted triplet state energies of thieno[2,3-*c*]-pyrroles **2a/b** were higher than that of isoindole **1**, the bond dissociation energies (BDEs) of the $\text{C}_\beta\text{-S}$ bond were estimated to be as low as ~ 48 kcal mol⁻¹ (see the SI for details). Considering the notorious instability of OPA-derived isoindoles,²³ we chose to focus on thieno[2,3-*c*]-pyrroles—species that are isoelectronic to isoindoles—as they were more stable and synthetically accessible through a similar 3CR.²⁴

Results and discussion

Validation of thieno[2,3-*c*]-pyrroles derived from Cys as useful precursors for generating L-alanyl radicals

Starting from *N*-benzoyl-L-cysteine methyl ester (BzCysOMe, **5**), ethanol amine and 2,3-thiophenedialdehyde, the corresponding thieno[2,3-*c*]-pyrroles **3** were synthesized in 78% yield as an

inseparable mixture of 2 isomers (Fig. S1a). Based on the UV-absorption spectrum (Fig. S1b), irradiation was performed at 365 nm using a 3S photoreactor (Fig. 2A). To our delight, **4** (BzAlaOMe) was obtained in 62% HPLC yield, indicating successful $\text{C}_\beta\text{-S}$ bond fragmentation; **5** (BzCysOMe) and its dimer (**6**) were detected in 14% and 18% yields, respectively, which may result from heterocycle–S bond homolysis in the excited state or oxidation of the thieno[2,3-*c*]-pyrrole core. Interestingly, no oxidation products of the primary carbon radical (*e.g.*, serine or dehydroalanine derivatives) were isolated, consistent with observations reported by Niu's group.¹³ Variations of thieno[2,3-*c*]-pyrroles were prepared and evaluated (Table S1), revealing that alkyl amines provided the optimal results.

Desulfurative transformations of cysteine on peptides

Following the successful proof-of-concept demonstration, we proceeded towards the desulfurative derivatization of cysteine-containing peptides. The tetrapeptide H-Val-Thr-Cys-Gly-OH (**7a**, VTCG), a cell attachment peptide,²⁵ was selected as a model substrate. The 3CR involving 2,3-thiophenedialdehyde and ethanolamine smoothly delivered the corresponding thieno[2,3-*c*]-pyrroles (see the SI for details). We were particularly intrigued by the potential to introduce modified or bioisosteric forms of endogenous amino acid residues, leveraging our late-stage derivatization strategy to bypass the need for *de novo* peptide synthesis. Initially, we examined 2-cyanoindole (**8**) as a radical trap to perform Giese-type addition following the 3CR in a one-pot fashion (Fig. 2B). Gratifyingly, **7b** was obtained in 44% HPLC yield (Fig. 2C, entry 1), which could be attributed to rearomatization *via* oxidation of the captodative radical intermediate.²⁶ Efforts to enhance the yield by changing the organic

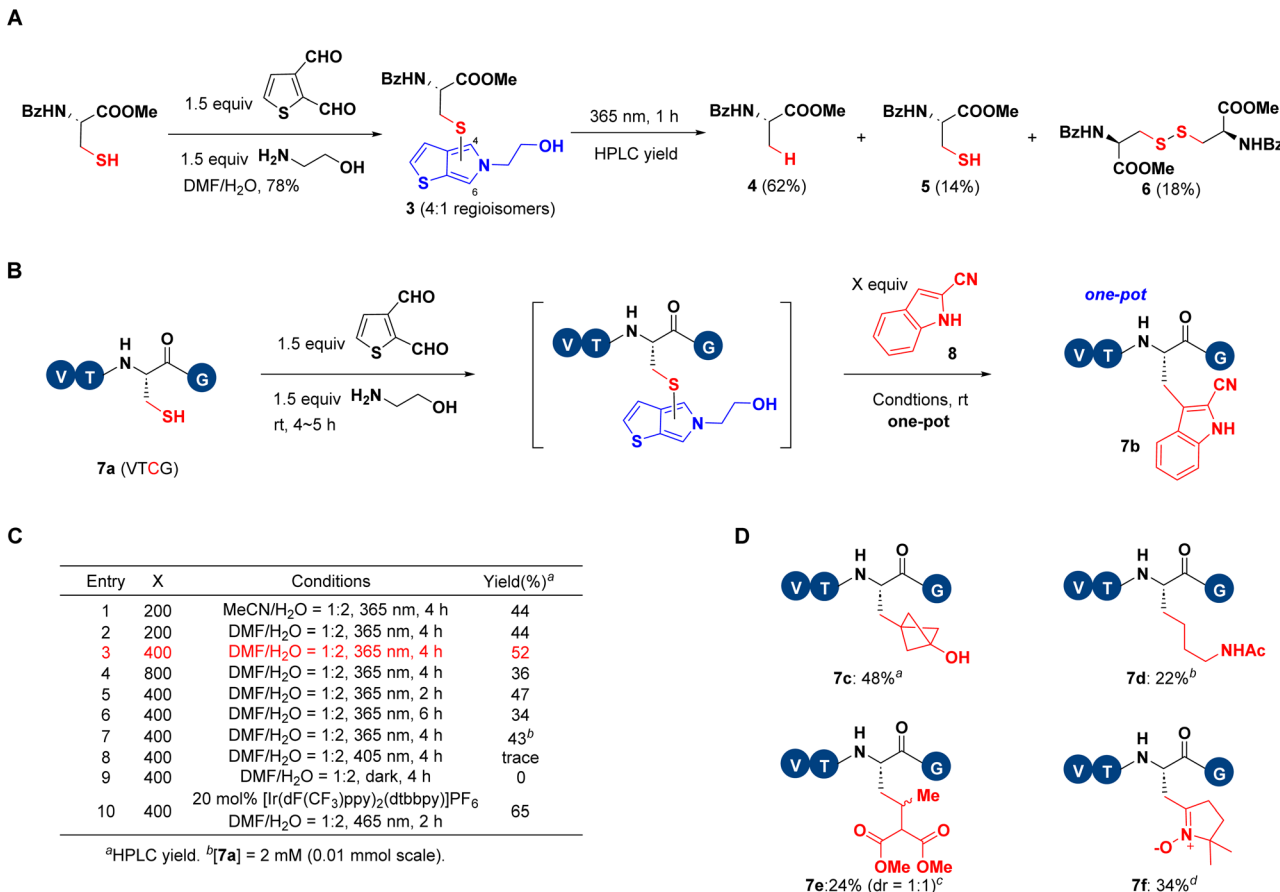


Fig. 2 Desulfurative transformations of cysteine on model substrates. (A) Photoreaction of the model thieno[2,3-c]-pyrrole. (B) One-pot transformation of cysteine to 2-cyanotryptophan on a model peptide (VTCG). (C) Optimization of the reaction conditions. After the 3CR ([7a] = 17 mM), the reaction mixture was diluted with the reaction solvent ([peptide] = 1 mM, 0.6 μ mol scale) followed by the addition of 8 and irradiation. (D) Products derived from VTCG (7a): (a) after the 3CR reaction in DMF/H₂O = 1:2 ([peptide] = 17 mM), the reaction mixture was diluted with DMF/H₂O = 1:4 ([peptide] = 1 mM, 200 equiv [1.1.1]propellane, 200 equiv B₂(cat)₂, 365 nm, rt, 4 h, then H₂O₂). (b) DMF/H₂O = 1:4, 200 equiv N-allylacetamide, 365 nm, rt, 4 h. (c) DMF/H₂O = 1:4, 200 equiv ethylenemalonate, 365 nm, rt, 4 h. (d) DMF/H₂O = 1:4, 200 equiv DMPO, 365 nm, rt, 4 h. All yields are isolated yields (0.01 mmol scale).

co-solvent from acetonitrile to DMF proved ineffective (entry 2). However, due to improved solubility of 2-cyanoindole (8) in the DMF/H₂O system, increasing its equivalency to 400 equiv in the 1 mM solution of the model peptide slightly improved the yield of 7b (entry 3). Doubling the 2-cyanoindole (8) equivalency proved unfruitful, likely due to competition for light absorption with thieno[2,3-c]-pyrroles (entry 4). Reaction monitoring indicated that the transformation was mostly complete within 2 hours (entry 5), with extended irradiation diminishing the yield, presumably due to the photodecomposition of 7b (entry 6). Increasing the reaction concentration slightly reduced efficiency of the transformation (entry 7). As expected, the reaction ceased upon a bathochromic shift or removal of the light source (entries 8 and 9). The utilization of photoredox catalysts in the photochemical step (Table S2), such as [Ir(dF(CF₃)ppy)₂(dtbbpy)]PF₆, accelerated the reaction and enabled its execution at a more bathochromic wavelength (entry 10). Nonetheless, we opted to conduct the reaction in the absence of the photocatalyst due to the side reactions in proteins commonly

observed in the photocatalysis systems, such as photoredox processes at unintended sites or singlet oxygen generation.^{11,27}

Having established a protocol for converting Cys into a mimic of tryptophan (Trp), we next considered the bioisostere of tryptophan (Tyr)—a hydrophobic residue with critical structural and bioactive roles,²⁸ and noted that the bicyclo[1.1.1]pentyl (BCP) moiety, recognized as a bioisostere of the *para*-substituted benzene ring,²⁹ could be accessed *via* the radical opening of [1,1,1]propellane.³⁰ Following the 3CR of 7a, irradiation of the reaction mixture with a 365 nm LED in the presence of 200 equiv of [1,1,1]propellane and bis(pinacolato)boron yielded the desired boronate; subsequent *in situ* oxidation with hydrogen peroxide afforded 7c in 48% isolated yield (Fig. 2D). Moreover, the L-alanyl C_B[·] radical generated using our protocol successfully reacted with previously reported radical traps. Under unoptimized conditions, 7a was converted to 7d bearing an N^{Ac} side chain in 22% yield by employing a large excess of N-allylacetamide during the photoreaction.^{10b} Similarly, the use of dimethyl ethylenemalonate and DMPO afforded 7e and 7f, respectively.³¹



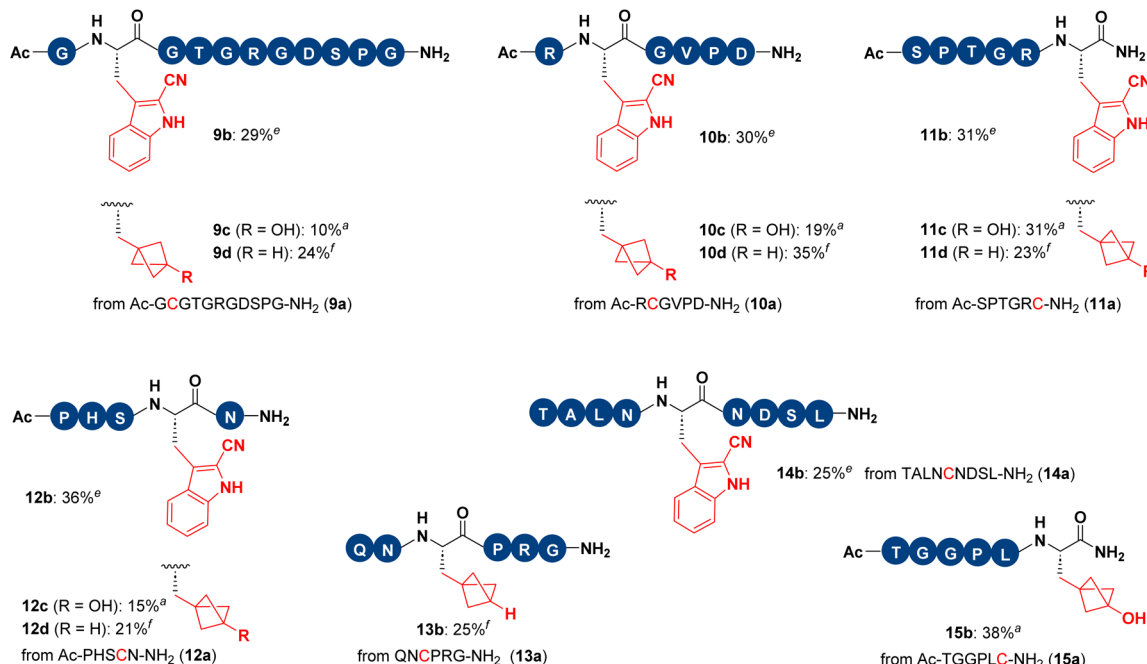


Fig. 3 Desulfurative transformations on catalog peptides. All yields are isolated yields (0.01 mmol scale). ^aAfter the 3CR reaction in DMF/H₂O = 1 : 2 ([peptide] = 17 mM), the reaction mixture was diluted with DMF/H₂O = 1 : 4 ([peptide] = 1 mM), 200 equiv [1.1.1]propellane, 200 equiv B₂(cat)₂, 365 nm, rt, 4 h, then H₂O₂. ^bDMF/H₂O = 1 : 4, 200 equiv N-allylacetamide, 365 nm, rt, 4 h. ^cDMF/H₂O = 1 : 4, 200 equiv ethylidene-malonate, 365 nm, rt, 4 h. ^dDMF/H₂O = 1 : 4, 200 equiv DMPO, 365 nm, rt, 4 h. ^eDMF/H₂O = 1 : 2, 400 equiv 8, 365 nm, rt, 4 h. ^fDMF/H₂O = 1 : 4, 200 equiv [1.1.1]propellane, 200 equiv B₂(cat)₂, 365 nm, rt, 4 h.

We further extended these desulfurative transformations to several other peptides (Fig. 3). An integrin binding peptide, **9a**,³² was successfully converted to **9b** and **9c**, while the radical opening of [1,1,1]propellane in the absence of bis(pinacolato) diboron produced **9d**, bearing the bicyclo[1.1.1]pentyl moiety mimicking the phenylalanine (Phe) residue. These reactions were also applicable to **10a** (an MMP-3 inhibitor),³³ **11a** (a sialic acid binding epitope),³⁴ **12a** (ATN-161, an integrin inhibitor),³⁵ **13a** (a vasopressin fragment),³⁶ nonapeptide **14a** (TALNCNDL),³⁷ and **15a** (a derivative of leucine-enkephalin).³⁸ These results demonstrate that the two-step, one-pot method enabled the conversion of Cys into modified or bioisosteric forms of tryptophan, tyrosine, and phenylalanine, even though the isolated yields were, at most, moderate.

Discovery of a new reagent to selectively install thieno[2,3-*c*]-pyrroles on Cys residues

While the unprotected N-terminal amino group did not interfere with the 3CR (peptides **13a** and **14a** in Fig. 3), significant interference from lysine residues was observed. The ε-amino group not only competes with thiols as a nucleophile,³⁹ but also rapidly reacts with 2,3-thiophenedialdehyde alone to form thieno[*c*]pyrrolones *via* a two-component reaction.^{24b,40} This side reaction could only be mitigated through intramolecular thiol capture or by using a large excess of intermolecular thiols. Li, Liu and co-workers addressed this issue by introducing high concentrations of guanidine, which resulted in the formation of a less reactive intermediate and enabled a stoichiometric

intermolecular OPA-amine-thiol 3CR on peptides.²¹ However, to selectively modify Cys residues with thieno[2,3-*c*]-pyrroles on native proteins—even in live cells under physiological conditions—there remains a pressing need for alternative reagents that circumvent lysine-related interference. To expand the scope of this chemical editing strategy to more physiologically relevant environments, we envisioned that thieno[2,3-*c*]-pyrroles could be installed at Cys residues through a substitution reaction rather than the three-component reaction (3CR).

We were intrigued by the 4- and 6-sulfonate derivatives of thieno[2,3-*c*]-pyrrole (**16a/b**, see Fig. S2 for their preparation), which have a counterpart derived from OPA that has been reported but not evaluated as a thiol-modifying reagent.⁴¹ Unlike electro-deficient heterocycles (e.g., sulfonylbenzothiazole, sulfonyloxadiazole, or sulfonylpyridines) that arylate Cys *via* the S_NAr mechanism,⁴² thieno[2,3-*c*]-pyrrole is an electronic-rich heterocycle. However, we observed spontaneous isomerization of **16a** and **16b** in deuterium oxide, leading to an equilibrium ratio of approximately 2 : 3 (Fig. 4A and S3), with deuteration occurring at the 6-H and 4-H positions on **16a** and **16b**, respectively.

The proposed mechanism for isomerization and deuteration involves protonation of **16a** to form **17a** and **18a**. Zwitterion **17a** could be trapped by bisulfite to give **19**, and subsequent elimination of 4-bisulfite generates **17b**, which undergoes deprotonation to yield **d-16b**. Deprotonation of **18a** results in **d-16a**. Addition of 1 equiv or 0.1 equiv of sodium bisulfite significantly accelerated the isomerization and



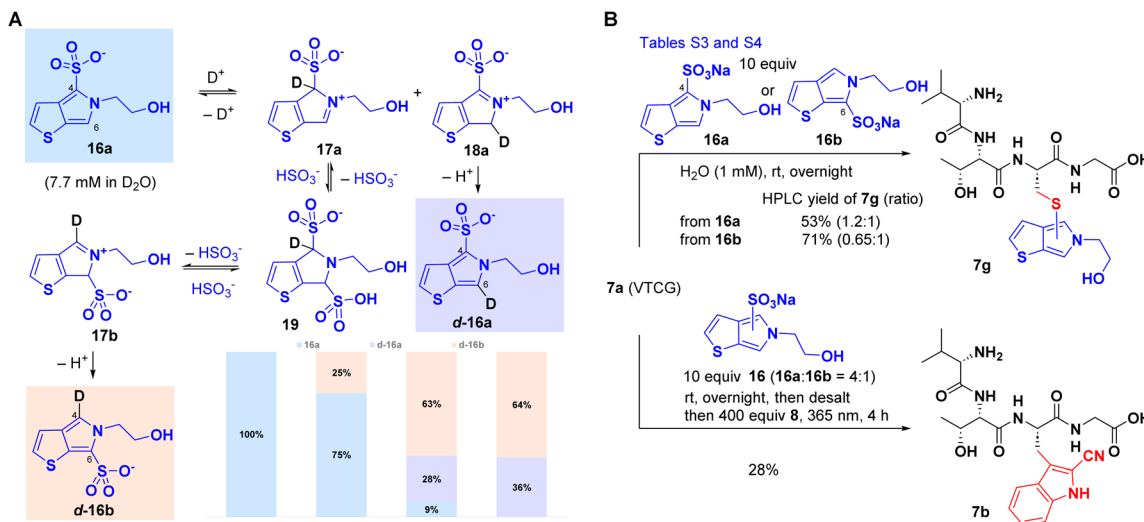


Fig. 4 Electrophilic Cys arylation with thieno[2,3-c]-pyrrole 4-sulfonate (16a) and 6-sulfonate (16b). (A) Isomerization and deuteration of 16a in D_2O at rt. (B) Installation of thieno[2,3-c]-pyrroles through sodium sulfonate reagents 16 and the subsequent photoreaction.

deuteration (Fig. S4–S7), presumably by lowering the pH (~ 5) and catalyzing the formation of **19**.

Although the detailed mechanism warrants further investigation, the presence of intermediates such as **17a**/**17b** suggests the formation of reactive species capable of engaging in nucleophilic addition with thiol groups within Cys, thereby installing the thieno[2,3-c]-pyrrole moiety following bisulfite elimination. Model peptide **7a** was used to evaluate conjugation efficiency under aqueous conditions (Tables S3 and S4). Due to challenges in assigning the regioisomers of product **7g**, the identities of the 4- and 6-regioisomers were not definitively determined. Both **16a** and **16b** afforded **7g** as mixtures of regioisomers, albeit in slightly different ratios, likely due to a concurrent isomerization process facilitated by the bisulfite byproduct (Fig. 4B). A robustness screen of the reaction between **7a** and **16** revealed that excess endogenous amino acids, including lysine, did not interfere with the installation of thieno[2,3-c]-pyrrole (Table S5),⁴³ supporting the chemoselectivity of Cys modification and paving the way for desulfurative Cys modification on proteins. Following the conjugation reaction of **7a** and desalting, the mixture was irradiated at 365 nm in the presence of **8**, leading to the formation of **7b** as the final product. Notably, a prolonged reaction time (overnight) and a large excess (10 equiv) of reagent **16** were required for adequate transformation of **7a**, indicating reduced reactivity relative to the 3CR-based method.

Cysteine labeling-desulfurization in cell lysates with **20**

We investigated the labeling profile of the thieno[2,3-c]-pyrrole reagent in the proteomes of mammalian cell lysates, which served as the initial step of our radical desulfurative transformations (Fig. 5A). To this end, cell lysates were incubated with increasing concentrations of **20**, an alkyne-functionalized probe, followed by biotin conjugation to probe-bound targets through copper-catalyzed azide–alkyne cycloaddition. Western

Blot (WB) analysis using Streptavidin-HRP revealed distinct labeling products (Fig. S8), indicating that the labeling abundance increased progressively with both the concentration of **20** and the incubation time, demonstrating a dose- and time-dependent response. Optimal labeling was achieved with a 5 mM concentration of **20** and a 6-hour incubation, which were used as the experimental parameters for subsequent investigations.

After conjugation with **20**, labeled proteins in cell lysates were subjected to click chemistry with a cleavable biotin linker, streptavidin pull-down, and trypsin digestion for identification (Fig. 5B). The modified peptides, which remained bound to the beads, were subsequently released by acid cleavage and analyzed by LC-MS/MS. Peptides exhibiting a mass shift of +302.1201 Da, corresponding to Cys modification, were identified as **20**-labeled peptides. Excluding proteins enriched in the DMSO group, a total of 1719 proteins were enriched, among which 27 peptide spectra corresponded to **20**-labeled peptides (Fig. 5C). The relatively low coverage (27 out of 1719) may stem from the anionic nature of **20**, which promotes non-specific enrichment of proteins *via* electrostatic interactions,⁴⁴ even in the absence of covalent modification. This limited detection of Cys-modified peptides (27) also aligns with the known lower reactivity of **16** compared to the 3CR approach and suggests a more selective reactivity profile, likely dictated by differences in Cys nucleophilicity. Such selectivity allows for targeted modification at a limited number of sites while leaving most Cys residues unmodified. For further analysis, we selected the peptide [R].CMPTFQFFK.[L] from thioredoxin (UniProt P10599), a ubiquitous disulfide reductase containing a CGPC active site that plays a pivotal role in maintaining cellular redox homeostasis and regulating key physiological processes such as cell proliferation, programmed cell death, and the oxidative stress response.⁴⁵ MS2 spectral analysis demonstrated high-confidence identification of the modified peptide, with a large

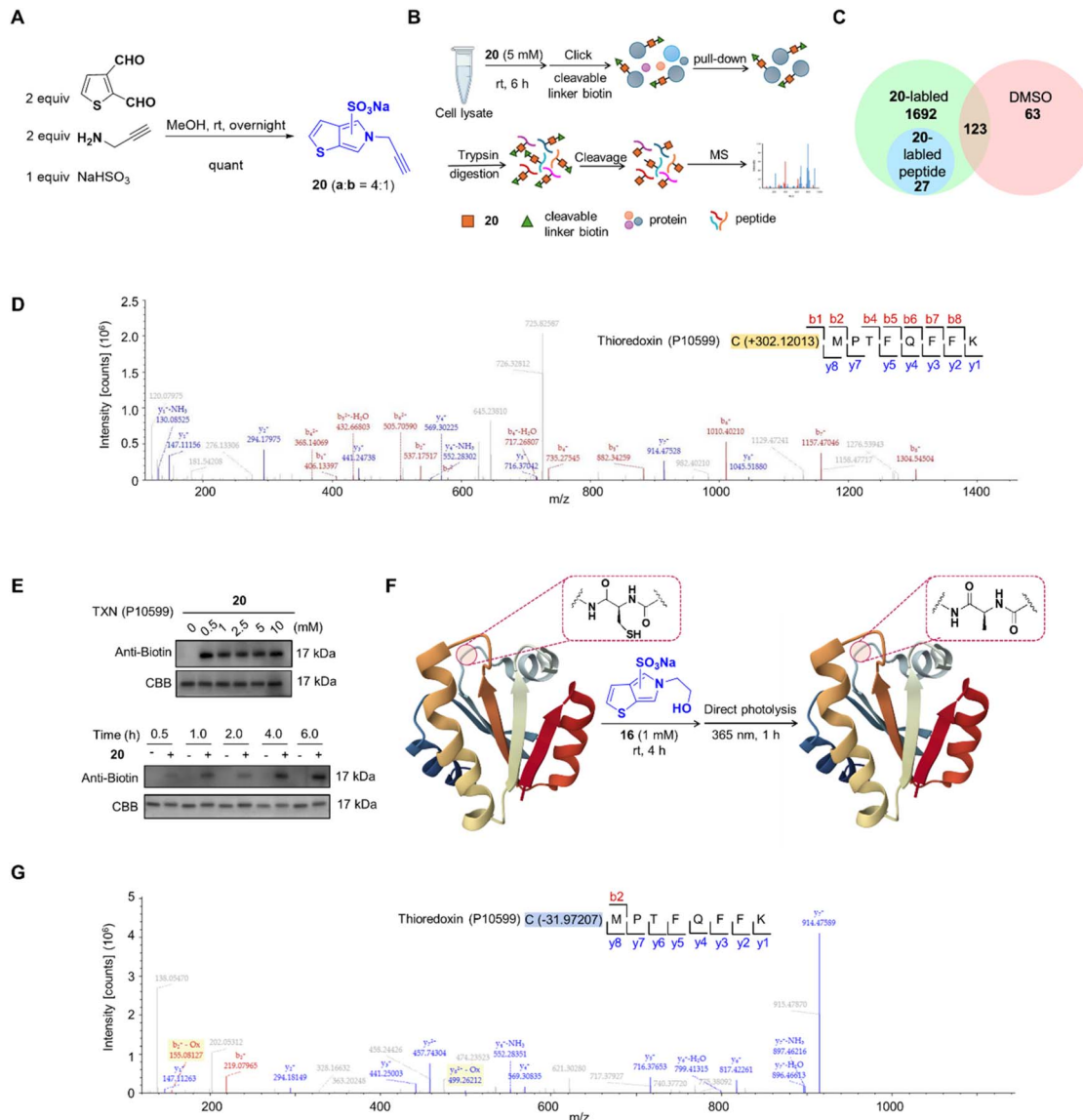


Fig. 5 Desulfurative modification of Cys residues in proteins. (A) Synthesis of the alkyne-functionalized probe **20**. (B) Workflow for identifying proteins labeled with thieno[2,3-*c*]-pyrrole. Cell lysates were incubated with **20**, enabling a click reaction with azide-labeled biotin for pull-down enrichment. Following trypsin catalysed hydrolysis and biotin cleavage, labeled proteins were identified and quantified by mass spectrometry (MS). (C) Venn diagram of the **20**-labeled proteomes in HEK293T cell lysates, quantified by nLC-MS/MS. (D) MS2 spectrum annotation of the thioredoxin site modified by **20**. The reaction with **20** adds a mass shift of +302.1201 Da to the modified cysteine residue. (E) Anti-biotin Western blot analysis of thioredoxin protein labeled with **20** at the indicated concentrations (upper) or for the indicated durations (lower). (F) Schematic representation of the desulfurative modification of cysteine residues in thioredoxin via **16** labeling and light irradiations (thioredoxin: PDB 1TRW). (G) MS2 spectrum annotation of **20**-induced desulfurative modification of cysteine residues in thioredoxin. The desulfurization decreases the mass by -31.9721 Da at the modified cysteine residue. CBB: coomassie brilliant blue.

fraction of matched y- and b-ions enabling precise localization of the modification (Fig. 5D).

Consequently, thioredoxin was selected for further studies. To assess labeling efficiency and optimize experimental conditions, thioredoxin was incubated with increasing concentrations of **20**. WB analysis using Streptavidin-HRP revealed clear labeling bands (Fig. 5E), indicating that labeling intensity increased in a dose- and time-dependent manner. Optimal labeling was achieved with 1 mM **20** and a 1-hour incubation, which were subsequently adopted as standard conditions for

further experiments (Fig. 5E). We next investigated whether compound **16** could promote desulfurization of cysteine residues in thioredoxin. Under the established conditions, thioredoxin was treated with 1 mM **16** at room temperature for 4 hours, followed by 1 hour of irradiation at 365 nm (Fig. 5F). LC-MS analysis revealed a mass shift of -31.9721 Da, consistent with cysteine desulfurization. MS2 spectra confirmed the high-confidence identification of the desulfurized product, with the Cys residue in the peptide [R].CMPTFQFFK.[L] exhibiting

a definitive desulfurization signature; this was further collaborated by the γ - and b -ion fragmentation data (Fig. 5G).

Proteome labeling in live cells and desulfurative modification of Cys residues in proteins

As previously discussed, the relatively low reactivity of **16** renders it well-suited for live-cell protein modification, minimizing interference with normal cellular physiology. Its sodium salt form also confers good water solubility, facilitating its use.

under biological conditions. Prior to live-cell application, we first accessed the effects of thieno[2,3-*c*]-pyrrole sulphonates and 365 nm irradiation on cell viability. Treatment with concentrations of **20** exceeding 10 mM inhibited HEK293T cell growth by approximately 50% within 1 hour, while no significant cytotoxicity was observed with shorter incubation times or 1-hour irradiation at 365 nm (Fig. S9). By treating HEK293 cells with varying concentrations and incubation times of **20**, followed by WB detection of labeled proteins, we determined that

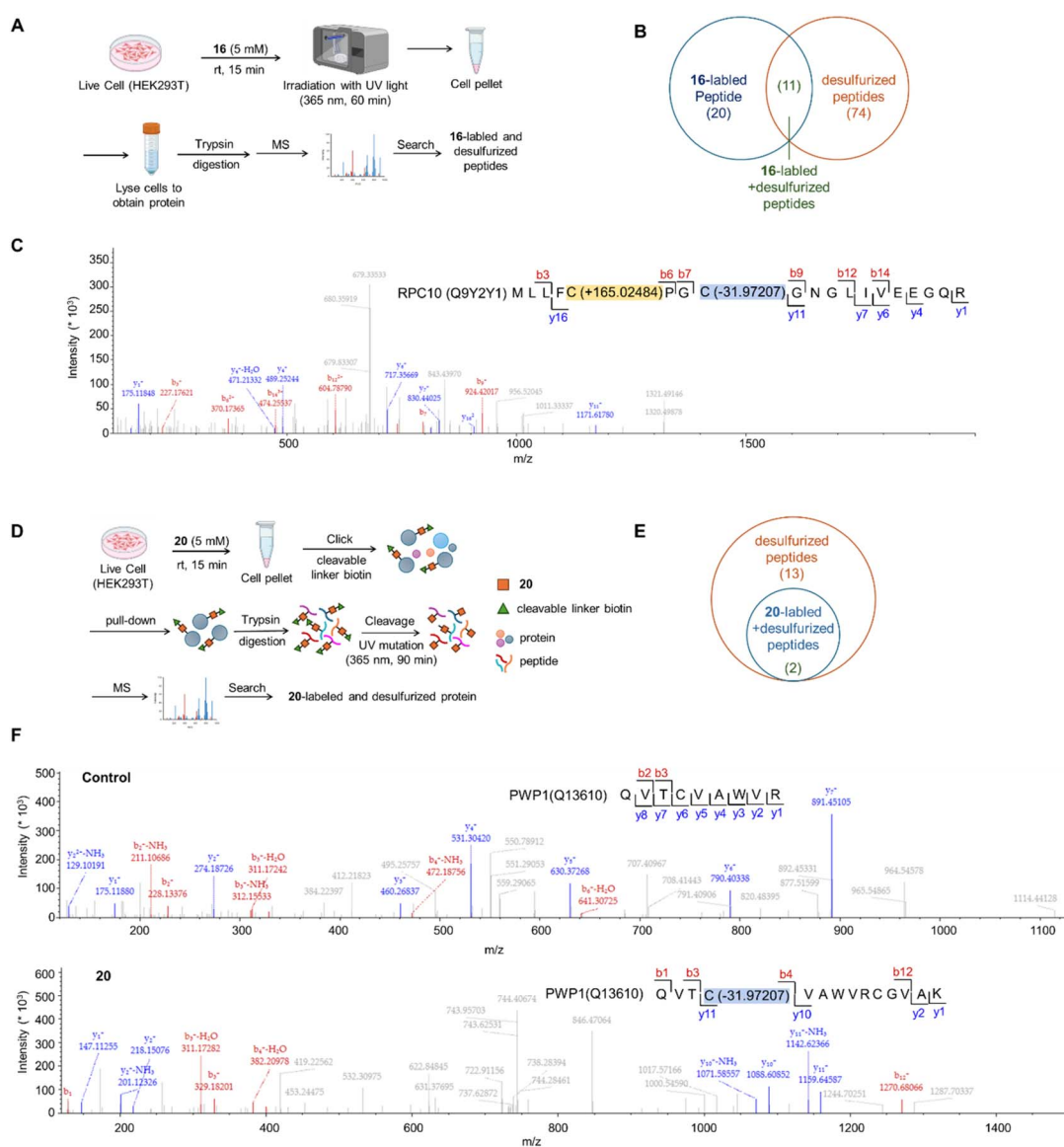


Fig. 6 Proteome labeling in live cells and desulfurative modification of Cys residues in proteins. (A) Workflow for identifying proteins labeled with **16** and modified by desulfuration of cysteine residues. HEK293T cells were treated with **16** (5 mM, 15 min), followed by light irradiation (365 nm, 60 min). The cells were lysed, and proteins were extracted for proteomic analysis via LC-MS/MS. (B) Venn diagram of the correlation number between **16**-labeled peptides and desulfurized peptides. (C) MS2 spectrum annotation of **16** labeling (+165.0248 Da) and desulfuration (−31.9721 Da) of cysteine residues in the RPC10 protein (UniProt Q9Y2Y1). (D) Workflow for identifying proteins labeled with **20** and modified by desulfuration of cysteine residues. HEK293T cells were labeled with **20** (5 mM, 15 min), followed by irradiation (365 nm, 60 min) for 1 hour. Cellular proteins were extracted and enriched by click chemistry using azide-labeled biotin for pull-down. After trypsin catalysed hydrolysis and biotin cleavage, labeled proteins were identified and quantified by nLC-MS/MS. (E) Venn diagram of the correlation number between **20**-labeled peptides and desulfurized peptides. (F) MS2 spectrum annotation of desulfuration modification (−31.9721 Da) in the PWP1 protein (UniProt Q13610).

optimal labeling was achieved with 5 mM **20** and a 15-minute incubation, conditions which were used as the experimental parameters for subsequent studies (Fig. S10).

HEK293T cells were labeled with 5 mM **16** for 15 minutes, followed by 60 minutes of irradiation at 365 nm (Fig. 6A). After lysis, extracted proteins underwent proteomic analysis *via* LC-MS/MS, revealing a mass shift of +165.0248 Da corresponding to **16**-labeled peptides, and a mass shift of -31.9721 Da indicative of desulfurative modification (Fig. S11). Identified peptides included those labeled with **16** (Table S7), desulfurized peptides (Table S8), and peptides exhibiting both labeling and desulfurization (Table S9). A Venn diagram depicted the correlation between **16**-labeled peptides and desulfurized peptides (Fig. 6B). Among these, the peptide [-]MLLFCPGCGNGLIVEEGQR.[C], from the DNA-directed RNA polymerase III subunit RPC10 (UniProt Q9Y2Y1), was both labeled with **16** and desulfurized at the same Cys-containing peptide. MS2 spectral analysis confirmed the presence of most y and b ions with high confidence, further validating the modification (Fig. 6C).

We also implemented a complementary detection strategy using **20**, which involved conjugating a cleavable biotin retrieval tag to protein targets *via* click chemistry, followed by neutravidin pull-down, and trypsin digestion (Fig. 6D). The modified peptides were then photocleaved and desulfurized (365 nm, 90 min) before LC-MS/MS analysis. A mass shifts of +259.0892 corresponded to **20**-labeled peptides, while a shift of -31.9721 Da indicated desulfurization. Identified peptides included those labeled with **20**, desulfurized peptides, and peptides exhibiting both labeling and desulfurization (Table S10). A Venn diagram depicted the correlation between **20**-labeled peptides and desulfurized peptides (Fig. 6E). The peptide [R].QVTCVAWVRCGVAK.[E], from the Periodic tryptophan protein 1 homolog (UniProt Q13610), exhibited the strongest intensity (>7-fold). MS2 spectral analysis of the **20**-labeled peptides confirmed the presence of numerous y and b ions with high confidence, further validating desulfurization at cysteine residues (Fig. 6F).

Finally, we verified the labeling and desulfurization of high-ionic-strength proteins. The MS2 analysis revealed that kielin/chordin-like protein (UniProt: Q6ZWJ8) and kelch-like protein 33 (UniProt: A6NCF5) underwent both labeling and desulfurization with high-confidence identification of the labeled and modified peptides (Fig. S12).

Conclusions

Reductive desulfurization serves as a valuable platform for peptide and protein modifications,⁴⁶ whereas the low natural abundance of Cys (2.2% in eukaryotes) contributes to inherent chemoselectivity.⁴⁷ As early as 1978, Clark and Lowe successfully used alkylation and photolysis to convert active-site Cys25 of papain into a serine or glycine residue.⁴⁸ We have developed a novel approach for site-specific cysteine modification and desulfurization in peptides and proteins, leveraging thieno[2,3-*c*]-pyrrole-based reagents and photochemical activation. The method doesn't require the use of a phosphine that disrupts disulfide bonds and strong electrophilic reagents, making it applicable for the selective targeting of free Cys residues under

mild conditions. The application of this strategy was demonstrated in both cell lysates and live mammalian cells, with successful labeling and desulfurization of proteins. Additionally, our method enabled the introduction of bioisosteric amino acid analogs even though the use of a large excess of radical trapping reagents prevented the direct application of the current approach in live cells.

Author contributions

Z. C. and W. W. contributed equally. The overall design of this project was conceptualized by T. L. and Z. C. with input from W. W., S.-C. C. and G. Z.; Z. C., B. C., and A. A. conducted the chemical experiments. W. W. performed the biological experiments. F. W. performed the computational studies. The manuscript was written and edited jointly by Z. C., W. W., and T. L. with feedback from other authors.

Conflicts of interest

There are no conflicts to declare.

Data availability

CCDC 2410369 (**S6**) contains the supplementary crystallographic data for this paper.⁴⁹

Supplementary information (SI): experimental procedures, characterization data, high-performance liquid chromatography (HPLC) procedures, and NMR spectra of all newly synthesized compounds, and coordinates for the density functional theory (DFT)-optimized structures (PDF). See DOI: <https://doi.org/10.1039/d5sc05199a>.

Acknowledgements

This work was supported by the National Natural Science Foundation of China (Grants 22425101 and 22171011), College of Chemistry and Molecular Engineering, Peking University, Beijing National Laboratory for Molecular Sciences, Peking-Tsinghua Center for Life Sciences, and Shenzhen Bay Laboratory. We thank Prof. Gang Li (Shenzhen Bay Laboratory) and Prof. Chu Wang (Peking University) for helpful discussions. The NMR, mass spectrometry, and XRD measurements were performed at the Analytical Instrumentation Center of Peking University. We acknowledge the assistance and support from PKUAC and support from the High-Performance Computing Platform of Peking University. We thank the Multi-Omics Mass Spectrometry Core of the Biomedical Research Core Facilities (BRCF) at the Shenzhen Bay Laboratory, for assistance with the mass spectrometry experiments and we are grateful to Dr Gongzheng Zhao and Dr Zheng Sun for their help with the analysis of the MS data. We acknowledge the assistance and support from the Peking University Chengdu Academy for Advanced Interdisciplinary Biotechnologies, Mass spectrometry platform, for assistance with the mass spectrometry experiments and we are grateful to Dr Xianghe Wang for his help with the analysis of the MS data.



References

1 N. J. Pace and E. Weerapana, *ACS Chem. Biol.*, 2023, **8**, 283.

2 P. E. Dawson, T. W. Muir, I. Clark-Lewis and S. B. H. Kent, *Science*, 1994, **266**, 776.

3 S. B. Gunnoo and A. Madder, *ChemBioChem*, 2016, **17**, 529.

4 T. H. Wright, M. R. J. Vallée and B. G. Davis, *Angew. Chem., Int. Ed.*, 2016, **55**, 5896.

5 F. W. Hoffmann, R. J. Ess, T. C. Simmons and R. S. Hanzel, *J. Am. Chem. Soc.*, 1956, **78**, 6414.

6 C. Walling and R. Rabinowitz, *J. Am. Chem. Soc.*, 1957, **79**, 5326.

7 Q. Wan and S. J. Danishefsky, *Angew. Chem., Int. Ed.*, 2007, **46**, 9248.

8 (a) Z. Sun, W. Ma, Y. Cao, T. Wei, X. Mo, H. Y. Chow, Y. Tan, *et al.*, *Chem*, 2022, **8**, 2542; (b) R. Desmet, C. Boidin-Wichlacz, R. Mhidia, A. Tasiemski, V. Agouridas and O. Melnyk, *Angew. Chem., Int. Ed.*, 2023, **62**, e202302648.

9 (a) X.-F. Gao, J.-J. Du, Z. Liu and J. Guo, *Org. Lett.*, 2016, **18**, 1166; (b) M. Lee, S. Neukirchen, C. Cabrele and O. Reiser, *J. Pept. Sci.*, 2017, **23**, 556; (c) C. Wan, D. Yang, X. Qin, Z. Xue, X. Guo, Z. Hou, C. Jiang, F. Yin, R. Wang and Z. Li, *Org. Biomol. Chem.*, 2022, **20**, 4105; (d) N. M. Venneti, G. Samala, R. M. I. Morsy, L. G. Mendoza, A. Isidro-Llobet, J. K. Tom, S. Mukherjee, M. E. Kopach and J. L. Stockdill, *J. Am. Chem. Soc.*, 2023, **145**, 1053; (e) D. Han, X. Deng, Y. Cui, X. Zhu, G. Deng, L.-J. Liang, G.-C. Chu and L. Liu, *Angew. Chem., Int. Ed.*, 2025, **64**, e202502884.

10 (a) R. C. Griffiths, F. R. Smith, J. E. Long, H. E. L. Williams, R. Layfield and N. J. Mitchell, *Angew. Chem., Int. Ed.*, 2020, **59**, 23659; (b) R. C. Griffiths, F. R. Smith, J. E. Long, D. Scott, H. E. L. Williams, N. J. Oldham, R. Layfield and N. J. Mitchell, *Angew. Chem., Int. Ed.*, 2022, **61**, e202110223.

11 Y. Nosaka and A. Y. Nosaka, *Chem. Rev.*, 2017, **117**, 11302.

12 (a) R. Jing, W. C. Powell, K. J. Fisch and M. A. Walczak, *J. Am. Chem. Soc.*, 2023, **145**, 22354; (b) R. Jing and M. A. Walczak, *Org. Lett.*, 2024, **26**, 2590.

13 Y. Wang, L.-F. Deng, X. Zhang, Z.-D. Mou and D. Niu, *Angew. Chem., Int. Ed.*, 2021, **60**, 2155.

14 C. E. Flitcroft, K. A. Jolliffe and C. S. P. McErlean, *Chem.-Eur. J.*, 2023, **29**, e202301083.

15 X.-P. Fu, Y. Yuan, A. Jha, N. Levin, A. M. Giltrap, J. Ren, D. Mamalis, S. Mohammed and B. G. Davis, *ACS Cent. Sci.*, 2023, **9**, 405.

16 (a) S.-C. Chen, Q. Zhu, Y. Cao, C. Li, Y. Guo, L. Kong and J. Che, *et al.*, *J. Am. Chem. Soc.*, 2021, **143**, 14046; (b) S.-C. Chen, Q. Zhu, H. Chen, Z. Chen and T. Luo, *Chem.-Eur. J.*, 2023, **29**, e202203425.

17 (a) M. Roth, *Anal. Chem.*, 1971, **43**, 880; (b) S. S. Simons and D. F. Johnson, *J. Am. Chem. Soc.*, 1976, **98**, 7098.

18 For a review, see: P. Zuman, *Chem. Rev.*, 2004, **104**, 3217.

19 A. V. Statsuk, D. J. Maly, M. A. Seeliger, M. A. Fabian, W. H. Biggs III., D. J. Lockhart, P. P. Zarrinkar, J. Kuriyan and K. M. Shokat, *J. Am. Chem. Soc.*, 2008, **130**, 17568.

20 (a) M. Todorovic, K. D. Schwab, J. Zeisler, C. Zhang, F. Bénard and D. M. Perrin, *Angew. Chem., Int. Ed.*, 2019, **58**, 14120; (b) Y. Zhang, Q. Zhang, C. T. T. Wong and X. Li, *J. Am. Chem. Soc.*, 2019, **141**, 12274.

21 C. H. P. Cheung, T. H. Chong, T. Wei, H. Liu and X. Li, *Angew. Chem., Int. Ed.*, 2023, **62**, e202217150.

22 R. W. Hoffman, *Chem. Rev.*, 1989, **89**, 1841.

23 C. M. Hong and A. V. Statsyuk, *Org. Biomol. Chem.*, 2013, **11**, 2932.

24 (a) V. A. Maslivets, J. J. La Clair and A. Kornienko, *RSC Adv.*, 2022, **12**, 6947; (b) T. Wei, D. Li, Y. Zhang, Y. Tang, H. Zhou, H. Liu and X. Li, *Small Methods*, 2022, **6**, 2201164.

25 K. A. Rich, F. W. I. V. George, J. L. Law and W. J. Martin, *Science*, 1990, **249**, 1574.

26 J. M. Lopchuk, W. L. Montgomery, J. P. Jasinski, S. Gorjifard and G. W. Gribble, *Tetrahedron Lett.*, 2013, **54**, 6142.

27 (a) H. Wang, W.-G. Li, K. Zeng, Y.-J. Wu, Y. Zhang, T.-L. Xu and Y. Chen, *Angew. Chem., Int. Ed.*, 2019, **58**, 561; (b) B. Josephson, C. Fehl, P. G. Isenegger, S. Nadal, T. H. Wright, A. W. J. Poh, B. J. Bower, A. M. Giltrap, L. Chen, C. Batchelor-McAuley, *et al.*, *Nature*, 2020, **585**, 530.

28 S. Koide and S. S. Sidhu, *ACS Chem. Biol.*, 2009, **4**, 325.

29 For a review, see: A. M. Dilmaç, E. Spulig, A. de Meijere and S. Bräse, *Angew. Chem., Int. Ed.*, 2017, **56**, 5684.

30 M. Messner, S. I. Kozhushkov and A. de Meijere, *Eur. J. Org. Chem.*, 2000, **2000**, 1137.

31 For an example of trapping of radicals by DMPO to afford nitrones, see: T. V. T. Nguyen, A. Bossonnet, M. D. Wodrich and J. Waser, *J. Am. Chem. Soc.*, 2023, **145**, 25411.

32 C. Cissé, S. V. Mathieu, M. B. O. Abeih, L. Flanagan, S. Vitale, P. Catty, D. Boturyn, I. Michaud-Soret and S. Crouzy, *ACS Chem. Biol.*, 2014, **9**, 2779.

33 N. Fotouhi, A. Lugo, M. Visnick, L. Lusch, R. Walsky, J. W. Coffey and A. C. Hanglow, *J. Biol. Chem.*, 1994, **269**, 30227.

34 L. D. Heerze, R. H. Smith, N. Wang and G. D. Armstrong, *Glycobiology*, 1995, **5**, 427.

35 N. Zhang, Y. Xia, Y. Zou, W. Yang, J. Zhang, Z. Zhong and F. Meng, *Mol. Pharmaceutics*, 2017, **14**, 2538.

36 J. P. H. Burbach, G. L. Kovacs, D. de Wied, J. W. van Nispen and H. M. Greven, *Science*, 1983, **221**, 1310.

37 A. Dondoni, A. Massi, P. Nanni and A. Roda, *Chem.-Eur. J.*, 2009, **15**, 11444.

38 J. Hughes, T. W. Smith, H. W. Kosterlitz, L. A. Fothergill, B. A. Morgan and H. R. Morris, *Nature*, 1975, **258**, 577.

39 X. Chu, B. Li, H.-Y. Liu, X. Sun, X. Yang, G. He, C. Zhou, W. Xuan, S.-L. Liu and G. Chen, *Angew. Chem., Int. Ed.*, 2023, **62**, e202212199.

40 (a) J. Thiele and J. Schneider, *Adv. Cycloaddit.*, 1909, **369**, 287; (b) C. L. Tung, C. T. T. Wong, E. Y. M. Fung and X. Li, *Org. Lett.*, 2016, **18**, 2600 and references cited therein.

41 (a) W. A. Jacobs, *J. Chromatogr.*, 1987, **392**, 435; (b) M. Maldonado and K. Maeyama, *Anal. Biochem.*, 2013, **432**, 1.

42 (a) D. Zhang, N. O. Devarie-Baez, Q. Li, J. R. Lancaster Jr. and M. Xian, *Org. Lett.*, 2012, **14**, 3396; (b) N. Toda, S. Asano and C. F. Barbas, *Angew. Chem., Int. Ed.*, 2013, **52**, 12592; (c) C. Zambaldo, E. V. Vinogradova, X. Qi, J. Iaconelli, R. M. Suci, M. Koh, K. Senkane and S. R. Chadwick, *et al.*



al., *J. Am. Chem. Soc.*, 2020, **142**, 8972; (d) B. M. Lipka, D. S. Honeycutt, G. M. Bassett, T. N. Kowal, M. Adamczyk, Z. C. Cartnick, V. M. Betti, J. M. Goldberg and F. Wang, *J. Am. Chem. Soc.*, 2023, **145**, 23427.

43 K. D. Collins and F. Glorius, *Nat. Chem.*, 2013, **5**, 597.

44 I. Capila and R. J. Linhardt, *Angew. Chem., Int. Ed.*, 2002, **41**, 390.

45 (a) E. S. J. Arnér and A. Holmgren, *Eur. J. Biochem.*, 2000, **267**, 6102; (b) J. Lu and H. Arne, *Free Radical Biol. Med.*, 2014, **66**, 75.

46 For reviews, see: (a) K. Jin and X. Li, *Chem.-Eur. J.*, 2018, **24**, 17397; (b) V. Agouridas, O. El Mahdi, V. Diemer, M. Cargoët, J.-C. M. Monbaliu and O. Melnyk, *Chem. Rev.*, 2019, **119**, 7328.

47 A. Miseta and P. Csutora, *Mol. Biol. Evol.*, 2000, **17**, 1232.

48 P. I. Clark and G. Lowe, *Eur. J. Biochem.*, 1978, **84**, 293.

49 CCDC 2410369 (S6): Experimental Crystal Structure Determination, 2025, DOI: [10.5517/ccdc.csd.cc2lx5vk](https://doi.org/10.5517/ccdc.csd.cc2lx5vk).

